NUMERICAL MODEL OF THE ATMOSPHERIC ADAPTIVE OPTICAL SYSTEM. I. LASER BEAM PROPAGATION IN THE ATMOSPHERE

V.P. Lukin, F.Yu. Kanev, P.A. Konyaev, and B.V. Fortes

Institute of Atmospheric Optics,
Siberian Branch of the Russian Academy of Sciences, Tomsk
Received September 27, 1994

We describe computational algorithms and computer programs which make it possible to simulate the propagation of high–power laser beams in the atmosphere as well as to assess the efficiency of application of different components of adaptive optical systems, namely, Hartmann wave–front sensors and flexible and segmented mirrors. The software developed may be used for the investigation of both the beam parameters and images formed through the atmosphere as well as for the design of adaptive optical systems.

1. INTRODUCTION

Numerical simulations of propagation of an optical wave through the atmosphere have become the basic techniques for investigation and design of optical systems that use high–power lasers. The first versions of computer programs for simulating thermal blooming appeared in early 1970s (Ref. 1). The subsequent versions came to describe the influence of atmospheric turbulence on beam formation in laser systems[2] and images in telescopes.[3] As the adaptive technology was developed, the computer programs came to involve the models of elements of the adaptive optical systems.[4]

This paper describes the computational algorithms used for creating packages of applied programs intended for modeling the adaptive control of laser beams in the atmosphere.

The computer programs we have developed allows us

– to create the scenario of laser beam propagation along the atmospheric path (horizontal, vertical, or slant);

– to assess the amplitude and phase distortions appearing in the beam propagating through the atmosphere;

– to determine the degree of efficiency of different ways used to minimize the arising distortions by the methods of adaptive optics.

The first part of the paper is devoted to numerical simulation of the process of high–power beam propagation in a moving randomly inhomogeneous absorbing gaseous medium such as clear turbulent atmosphere. The models of altitude profiles of accompanying atmospheric parameters are also presented.

In the second part of the paper, the algorithms are described, which simulate the elements of adaptive optical systems, including a Hartmann wave–front sensor and different variants of wave–front correctors.

The third part of the paper describes the interface of the entire program package which is written in FORTRAN and operates in MS DOS and WINDOWS environment.

The created software can be used for investigation of the intensity fluctuations and of the optical wave phase in the atmosphere, simulation of thermal blooming of high–power laser beams, and image formation in telescopes as well as for investigation of the efficiency and design of adaptive optical systems.

2. LASER BEAM PROPAGATION

Computer simulation of the process of laser beam propagation in an inhomogeneous medium is based on the numerical solution of the wave equation written in the parabolic approximation for the scalar complex amplitude U of the beam and the field of the medium refractive index, n:

$$2\, i\, k\, \frac{\partial U}{\partial z} = \Delta_{\perp} U + k^2 n\,(T)\, U, \tag{1}$$

where z is the direction of the beam propagation, $k = 2\pi/\lambda$ is the wave number (λ is the wavelength). To obtain a particular solution, Eq. (1) is supplemented with the boundary conditions for the complex field amplitude in the cross section of emitting aperture and by the initial conditions for the refractive index field.

When simulating the dynamic and nonlinear problems we need for simultaneous numerical solution of Eq. (1) and a material equation describing the change of medium state in time. At present the splitting method together with the fast Fourier transform (FFT) algorithm is the most effective and reliable method for numerical solution of evolution equations.

In our calculations we use a modified splitting method[5] and the FFT algorithm using mixed basis.[6]

3. NONSTATIONARY THERMAL BLOOMING

At thermal blooming the medium refractive index varies because of medium heat due to absorption of a laser radiation. As a rule, in these problems the temperature dependence of the refractive index is assumed to be linear:

$$n = n'_T\, T(x, y)$$

Time evolution of the temperature field $T(x, y, t)$ in the dynamic turbulent atmosphere is described by the material equation

$$\frac{\partial T}{\partial t} = \chi \frac{\partial^2 T}{\partial^2 x} + \chi \frac{\partial^2 T}{\partial^2 y} - V_x \frac{\partial T}{\partial x} - V_y \frac{\partial T}{\partial y} + \frac{\alpha}{\rho\, C_p} I, \tag{2}$$

where t is time, χ is the coefficient of thermal conductivity, V_x and V_y are the transverse components of wind velocity, α is the medium absorption coefficient, ρ is the medium

0235-6880/95/03 210-05 $02.00 © 1995 Institute of Atmospheric Optics

density, C_p is the specific heat of the medium, and I is the laser radiation intensity.

The coefficients in Eq. (2) may depend on the longitudinal coordinate z (along vertical and slant paths) and also vary randomly (for example, space–time fluctuations of the wind velocity V). Moreover, at the initial point in time the temperature field T can be a random function of coordinates x, y, and z (atmospheric turbulence).

For numerical solution of Eq. (2) we use the following difference approximation of the diffusion and convection terms:

$$\chi\, T^{-}_{xx} + \chi\, T^{-}_{yy} - V^{+}_{x}\, T^{-}_{x} - V^{-}_{x}\, T_{x} - V^{+}_{y}\, T^{-}_{y} - V^{-}_{y}\, T_{y}\ ,$$

where

$$T_{x} = (T(i+1, j) - T(i, j)) / h;\ i = 1,\ n-1;\ j = 1,\ n,$$

$$T^{-}_{x} = (T(i, j) - T(i-1, j)) / h;\ i = 2,\ n;\ j = 1,\ n;$$

$$V^{\pm} = 1/2\,(V \pm |V|)$$

for the difference approximations of a derivative with respect to the x–direction and analogous approximations for the y–direction.

Now we can write Eq. (2) in the difference form

$$\frac{\partial T_{ij}}{\partial t} = T_{x}\left(\frac{\chi}{h} - V^{-}_{x}\right) - T_{x}\left(\frac{\chi}{h} + V^{+}_{x}\right) + T_{y}\left(\frac{\chi}{h} - V^{-}_{y}\right) - T_{y}\left(\frac{\chi}{h} + V^{+}_{y}\right) + \frac{\alpha}{\rho\, C_{p}}\, I$$

for $i = 2,\ n-1;\ j = 2,\ n-1$ under the boundary conditions $T_{ij} = 0$.

Dividing the step in time Δt into two half–steps we obtain

$$\frac{T^{m+1/2} - T^{m}}{\Delta t / 2} = V_{Rt}\, T^{m+1/2}_{x} - V_{Lf}\, T^{m+1/2}_{x} + V_{Up}\, T^{m}_{y} - V_{Dn}\, T^{m}_{y} + \frac{\alpha}{\rho\, C_{p}}\, I;$$

$$\frac{T^{m+1} - T^{m+1/2}}{\Delta t / 2} = V_{Rt}\, T^{m+1/2}_{x} - V_{Lf}\, T^{m+1/2}_{x} + V_{Up}\, T^{m+1}_{y} - V_{Dn}\, T^{m+1}_{y} + \frac{\alpha}{\rho\, C_{p}}\, I,$$

where the superscript m denotes the number of a temporal layer and

$$V_{Rt} = \chi / h - V^{-}_{x},\qquad V_{Lf} = \chi / h + V^{+}_{x};$$

$$V_{Up} = \chi / h - V^{-}_{y},\qquad V_{Dn} = \chi / h + V^{+}_{y}.$$

The equations obtained can be written in the canonical form:

$$A\, T^{m+1/2}_{i-1,\, j} - C\, T^{m+1/2}_{i,\, j} + B\, T^{m+1/2}_{i+1,\, j} = -F_{i},$$

$$A = V_{Lf};\quad B = V_{Rt};\quad C = 2 / \Delta t + A + B;$$

$$F_{i} = 2 / \Delta t\, T^{m}_{i,\, j} + V_{Up}\, T^{m}_{y} - V_{Dn}\, T^{m}_{y} + \frac{\alpha}{\rho\, C_{p}}\, I$$

and

$$A\, T^{m+1}_{i,\, j-1} - C\, T^{m+1}_{i,\, j} + B\, T^{m+1}_{i,\, j+1} = -F_{j},$$

$$A = V_{Dn};\quad B = V_{Up};\quad C = 2 / \Delta t + A + B;$$

$$F_{j} = 2 / \Delta t\, T^{m+1/2}_{i,\, j} + V_{Rt}\, T^{m+1/2}_{x} - V_{Lf}\, T^{m+1/2}_{x} + \frac{\alpha}{\rho\, C_{p}}\, I.$$

Thus we have obtained two sets of linear equations. The sets of equations can be solved using the following procedure (formulas are given for the first set of equations).

1) Forward run:

$$\alpha_{1}=0;\ \alpha_{2}=B/C;\ \alpha_{i}=B/(C-A\alpha_{i-1}),\ i=3,\ n-1,\ \alpha_{n}=0;$$

$$\beta_{1}=0;\ \beta_{i} = F_{i} + A\, \beta_{i-1} / (C - A\, \alpha_{i-1}),\ i = 2,\ n-1.$$

2) Reverse run:

$$T^{m+1/2}_{n,\, j} = 0;\ T^{m+1/2}_{i,\, j} = \beta_{i} + \alpha_{i}\, T^{m+1/2}_{i+1,\, j};\ i = n-1,\ 2;$$

$$T^{m+1/2}_{1,\, j} = 0.$$

Thus, the proposed algorithm makes it possible to simulate the evolution of the temperature field taking into account two mechanisms, namely, forced convection (at an arbitrary direction of wind) and molecular thermal conductivity, that is important with the presence of stagnation zones along the beam propagation path.

4. SIMULATION OF ATMOSPHERIC TURBULENCE

To take into account the influence of turbulent fluctuations of the atmospheric refractive index on the propagation of a laser beam, it is necessary to simulate a two–dimensional randomly inhomogeneous phase distortions of the wave front with the corresponding spectral power density

$$F_{s}(\kappa) = 2\pi\, L\, k^{2}\, \Phi_{n}(\kappa),$$

where $\Phi_{n}(\kappa) = 0{,}033\, C^{2}_{n}\, (\kappa^{2} + \kappa^{2}_{0})^{-11/6}$ is the spectral power density of the refractive index; $\kappa_{0} = 2\pi/L_{0}$, L_{0} is the outer scale of turbulence. For an inhomogeneous paths this expression takes the form

$$F_{s}(\kappa) = 0{,}489\, r_{0}^{-5/9}\, \Phi(\kappa),$$

where

$$\Phi(\kappa) = \Phi_{n}(\kappa) / (0{,}033\, C^{2}_{n}),$$

and the Fried coherence radius r_0 in a general case of a slant path is calculated as

$$r_{0} = \left(0{,}423\, k^{2}\, \sec(a) \int\limits_{h_{1}}^{h_{2}} C^{2}_{n}(h)\, \mathrm{d}\, h\right)^{-3/5},$$

where α is the zenith angle, h_1 and h_2 are the altitudes of the upper and the lower boundaries of the atmospheric layer.

Let us consider the complex spectral amplitudes $A_s(\kappa)$ of a random phase function $S(x, y) = S(\rho)$. The phase $S(\rho)$ and its spectral amplitude are related by the two–dimensional Fourier transforms:

$$A_{s}(\kappa) = 1 / (2\,\pi)^{2} \int\int \mathrm{d}^{2}\,\rho\, S(\rho)\, \exp\,(i\,\kappa\,\rho);$$

$$S(\rho) = \int\int \mathrm{d}^{2}\,\kappa\, A(\kappa)\, \exp\,(-\,i\,\kappa\,\rho),$$

and the spectral density $F_s(\kappa)$ is equal to the average square of the spectral amplitude modulus:

$$F_{s}(\kappa) = \langle |A_{s}(\kappa)|^{2} \rangle.$$

Since the required phase function S should be real, its Fourier transform must satisfy the condition

$$A_s(-\kappa) = A_s^*(\kappa),$$

where the asterisk * means the operation of the complex conjugation. It should be noted that the one–dimensional Fourier transform of this expression gives

$$A_x(x, -\kappa_y) = A_x^*(x, \kappa_y),$$

in the x–direction, where

$$A_x(x, \kappa_y) = \int \mathrm{d}\,\kappa_x\, A_s(\kappa_x, \kappa_y) \exp(i\,\kappa_x\, x).$$

Thus, we can calculate the x–Fourier transform only for $\kappa_y \geq 0$ and then obtain the values $A_x(x, \kappa_y)$ for $\kappa_y < 0$ using the symmetry property. Note also that

$$A_s(-\kappa_x, 0) = A_s^*(\kappa_x, 0).$$

At numerical simulation of random phase distortions using a computer we approximate the field $S(\rho)$ by means of a two–dimensional real data array $S(i, j)$ so that

$$S(x, y) = S(I\,\Delta x, J\,\Delta y) = S_{IJ}.$$

We also assume that $S(x, y)$ is a periodic function over both variables with the periods $n\Delta x$ and $n\Delta y$. Thus, we can change the Fourier integral for a discrete sum

$$S_{IJ} = \sum_{K,\, L=1,\, n} \sum A_{KL} \exp(i(K-1)\Delta\kappa_x I\Delta x)\exp(i(L-1)\Delta\kappa_y J\Delta y),$$

where $\Delta\kappa_x = 2\pi/(n\Delta x)$, $\Delta\kappa_y = 2\pi/(n\Delta y)$. Assuming $\Delta x = \Delta y = h$ we obtain

$$S_{IJ} = \sum_{K,\, L=1,\, n} \sum A_{KL} \exp\left(i\,\frac{2\pi}{n}\,(I\,(K-1) + J\,(L-1))\right).$$

For making calculation with the use of the formula obtained we apply the FFT algorithm using a mixed base.

There are some methods of initialization of the data array A. The real and imaginary parts of the data array are usually packed by independent random numbers, distributed either uniformly or normally so that the condition

$$<|A_{KL}|^2> = F_s(\kappa_K, \kappa_L)\,\Delta\kappa^2,$$

holds, where $\kappa_K = (K-1)\,\Delta\kappa$ and $\kappa_L = (L-1)\,\Delta\kappa$.

We use the following expression for initializing the A data array:

$$A_{KL} = (F_s(\kappa_K, \kappa_L)\,\Delta\kappa^2)^{1/2} \exp(2\pi\, i\, RND),$$

where RND is random number uniformly distributed over the interval [0, 1].

To simulate the dynamic problems dealing with time evolution of turbulent distortions, we have used the hypothesis of "the frozen turbulence". The phase screen shift in the direction of the wind vector **V** by the value $t\,V$ is observed, where t is the current time. Using the "repetition" property of program generators of pseudo–random numbers we generate a set of phase screens imitating a randomly inhomogeneous medium at every next moment according to the following rule:

$$A_{KL} = (F_s(\kappa_K, \kappa_L)\Delta\kappa^2)^{1/2} \exp(i[2\pi RND + \kappa_K S_x + \kappa_L S_y]),$$

where $S_x = V_x\, t$ and $S_y = V_y\, t$ are the shifts along the x and y directions.

The advantage of this approach is evident since we have no need for large data arrays to be stored in the computer memory.

General formula for spatial frequencies in accordance with indexing of data arrays in the FFT algorithm is of the form:

$$\kappa_K = \Delta\kappa(K-1), \text{ if } K \leq Nq; \text{ otherwise } \kappa_K = \Delta\kappa(K-1-n)$$

$$\kappa_L = \Delta\kappa(L-1), \text{ if } L \leq Nq; \text{ otherwise } \kappa_L = \Delta\kappa(L-1-n)$$

$Nq = 1 + [n/2]$, where the brackets mean the integer part of a number.

It is easy to modify the method described for solving the problems sensitive to the shape of spectral density F_s. For example, in order to take into account the influence of inner and outer scales of turbulence we use the parameters $R_{\max}$ and $R_{\min}$ limiting the shape of spectral density within the range of spatial frequencies $[2\pi/R_{\max}, 2\pi/R_{\min}]$ (Ref. 7).

5. SCENARIOS OF THE NUMERICAL EXPERIMENT

The conditions of laser beam propagation in the atmosphere include such characteristics as the laser source location, location and motion characteristics of a radiation detector. Figure 1 shows one of the possible scenarios of the numerical experiment.

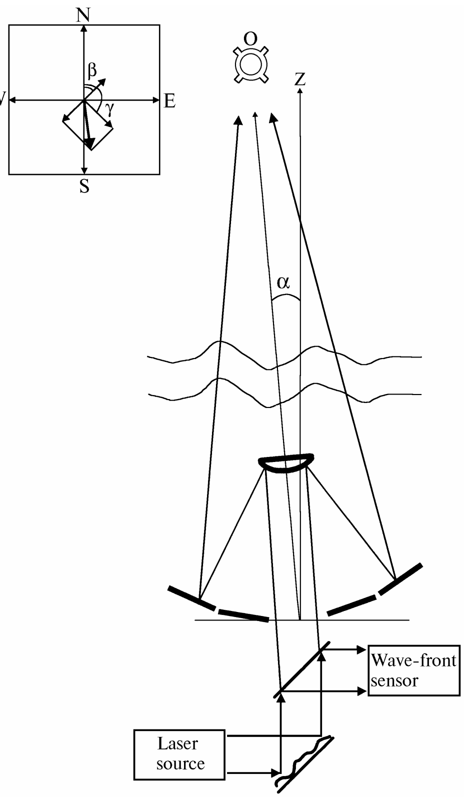

FIG. 1. Scheme of the experiment simulated numerically (construction of an image of a remote object O *with the use of an adaptive telescope):* α *is the receiver zenith angle,* β *is the scanning angle, and* γ *is the wind direction.*

A number of layers in the atmospheric model is fixed and equals 30. Vertical profiles of the basic thermodynamic parameters are given in the form of table values with a 1–km step up to the altitude of 30 km (if necessary, we use spline interpolation). The midlatitude atmospheric models are created for two seasons (winter and summer), three wavelengths ($\lambda = 1.06$, 3.15, and 10.6 μm) and three turbulent conditions (the best, intermediate, and the worst).

Altitude of the laser source h_0, the initial beam radius a_0, radiation intensity at the beam axis, I_0, and intensity profile in the cross section determine the source characteristics. Detector altitude, zenith angle of the propagation path, azimuth, and scanning speed determine the detector characteristics.

The profile components of the effective wind velocity with regard to the detector travel direction and speed are calculated by the following formulas:

$$V_x(h) = V(h)\sin\gamma - V_t \sin\beta\, (h - h_0)/(h_t - h_0)\ ;$$

$$V_y(h) = V(h)\cos\gamma - V_t \cos\beta\, (h - h_0)/(h_t - h_0),$$

where β is the angle of the detector velocity (in radians); γ is the wind velocity angle (in radians); V_t is the detector movement speed, and $V(h)$ is the wind velocity profile.

As a scale factor for the intensity of radiation from source we use the characteristic power density calculated by the formula:

$$P_k(h) = \rho(h)\, C_p\, V_s(h)\, T_0/(\alpha_m(h) + \alpha_a(h)),$$

where

$$V_s(h) = (V_x(h)^2 + V_y(h)^2)^{1/2}.$$

Then the vertical profile of the nonlinearity parameter normalized to its value at the Earth's surface can be determined as $R(h) = P_k(0)/P_k(h)$.

The Fried coherence radius, used at simulating the atmospheric turbulence, is calculated by the vertical profile of structural characteristic $C_n^2(h)$ for three turbulent conditions taking into account the wavelength of radiation emitted from a source.

6. ATMOSPHERIC MODELS

To consider the vertical variability of atmospheric parameters entering into Eqs. (1) and (2), we have used the standard atmospheric models allowing for physical and geographical conditions and constructed on the basis of the long–term statistical measurements of space–time variations of meteorological parameters.[8–13]

The atmospheric air is assumed to be an ideal gas with constant composition and the following equations of state

$$P = \rho R T \qquad (3)$$

and static equilibrium

$$-\, d P = \rho g\, d h\ , \qquad (4)$$

where P is the pressure; ρ is the density; R is the universal gas constant; T is the temperature; g is the acceleration due to gravity; h is the geometric height.

Profiles of temperature, pressure, and air density

In accordance with the character of temperature variations with altitude the atmosphere can be divided into the following layers: troposphere, stratosphere, mesosphere, and thermosphere. The altitude profile of temperature within each specific layer is approximated by a linear function of the geopotential altitude H

$$T = T_* + \beta\, (H - H_*), \qquad (5)$$

where T_* and H_* are the values of temperature and geopotential altitude of the lower boundary of the atmospheric layer under study; $\beta = \mathrm{d}T/\mathrm{d}H$ is the temperature lapse rate with respect to the geopotential altitude H:

$$H = h\, r/(r + h),$$

where r is the Earth's radius.

The values of T_*, H_*, and β, used in our calculations, can be found in Ref. 10.

Joint solution of Eqs. (3) and (4) taking into account Eq. (5) gives the following expressions for the altitude profile of pressure:

$$\begin{aligned} P &= P_*[1 + \beta/T_*(H - H_*)]^{-g/\beta R} \quad \text{at } \beta \neq 0,\\ P &= P_*\exp[-\, g/RT_*(H - H_*)] \quad \text{at } \beta = 0. \end{aligned} \qquad (6)$$

The vertical profile of air density is calculated using the given temperature (5) and pressure (6) profiles by the equation of state (3).

Profiles of wind velocity

Owing to a considerable space–time variation of wind in the atmosphere the data of routine atmospheric sounding should be used when solving the applied problems. However, for estimating the efficiency of adaptive optical systems, intended for operation in the atmosphere, it is sufficient to use the models of wind structure obtained by averaging the long–term data from sounding stations such as the zonal (latitude) component V_x, the meridian component V_y, the modulus of the wind velocity vector V_s, and the resulting wind V_r. The values of these characteristics for midlatitude summer and winter atmospheric models are taken from Ref. 10 and used when constructing the altitude profile of the nonlinearity parameter. In this case we take into account the relationships between these characteristics

$$V_x = V_s \sin\gamma;\ V_y = V_s \cos\gamma;$$

$$V_r = (\langle V_x\rangle^2 + \langle V_y\rangle^2)^{1/2};\ \gamma = \arctan\,(V_x\ /\ V_y),$$

where γ is the angle between the meridian of observation point and wind direction.

To study the influence of fluctuations of the wind speed and direction on the instability of operation of systems of phase conjugation of a reference wave, the data on rms deviations of wind characteristics from Ref. 10 are also included into the model of wind structure used.

Profiles of turbulence structure characteristic

According to Kolmogorov–Obukhov hypothesis, in the inertial interval $l_0 < r < L_0$ the structure function of the refractive index fluctuations obeys the law

$$D_n(r) = C_n^2\, r^{2/3}.$$

In the free atmosphere the ratio of the outer scale L_0 to the inner scale l_0 of turbulence can reach several orders of magnitude. In numerical simulation the value of the inertial interval is limited by the size of the computer calculation grid. As a rule, the ratio L_0/l_0 in the numerical experiment does not exceed 1000.

The structure characteristic C_n^2, governing the intensity of turbulent distortions, varies with the altitude as h^{-a} in the ground layer ($h < 20$ m) ($a = 4/3$ for a free convection, $a = 2/3$ for a neutral stratification, $a = 0$ for stable stratification).

In the free atmosphere the character of altitude dependence of C_n^2 varies with varying meteorological situations that makes it difficult to create any universal model. We use a simple empirical model obtained on the basis of experimental data (up to 20 km) from Ref. 11:

– for the best conditions

$$\log [C_n^2 \min(z) - 5.19 \cdot 10^{-16} \cdot 10^{-0.86} z] = - 18.34 + 0.29\, z + + 8.84 \cdot 10^{-2}\, z^2 + 7.43 \cdot 10^{-4}\, z^3;$$

– for the worst conditions

$$\log [C_n^2 \max(z) - 9.5 \cdot 10^{-14} \cdot 10^{-2.09} z] = - 14.39 + 0.17\, z - - 3.48 \cdot 10^{-2}\, z^2 + 9.59 \cdot 10^{-4}\, z^3;$$

– for intermediate conditions

$$[\log C_n^2(z)]_{\rm av} = 1/2 \{\log [C_n^2 \max(z)] + \log [C_n^2 \min(z)]\}.$$

The values of h are given in kilometers, so C_n^2 is measured in $m^{-2/3}$.

Profiles of molecular and aerosol absorption

As known, molecular absorption of radiation is strongly dependent on the radiation frequency. At present the most universal and accurate method for calculating the absorption characteristics is the line–by–line account for contributions to the absorption at the frequency of each line. We have used the data from Ref. 12, obtained in the numerical calculations up to 20–km altitudes with a 1–km step for the wavelengths $\lambda = 1.06$, 1.315, and 10.6 μm.

Atmospheric aerosol also can make an important contribution to the thermal blooming of high–power radiation in addition to the absorption by gases of the atmospheric air. To account for this contribution we have used the data on altitude profiles of aerosol absorption from Ref. 13.

REFERENCES

1. L.C. Bradley and J. Herrmann, J. Opt. Soc. Am. **61**, No. 5, 668 (1971).
2. J.A. Fleck, J.R. Morris, and M.D. Feit, Appl. Phys. **10**, No. 1, 129–139 (1976).
3. R.A. Muller and A. Buffington, J. Opt. Soc. Am. **64**, No. 9, 1200–1210 (1974).
4. R. Cubalchini, J. Opt. Soc. Am. **69**, No. 7, 972–977 (1979).
5. P.A. Konyaev, *"Numerical study of thermal distortions of laser beams in the atmosphere,"* Candidate's Dissertation in Physical and Mathematical Sciences, Tomsk (1984).
6. R. Singleton, IEEE Transactions on Audio and Electroacoustics **AU–17**, No. 2, 93–103 (1969).
7. B.V. Fortes and V.P. Lukin, Proc. SPIE **1668**, 477–488 (1992).
8. *Standard Atmosphere. Parameters.* GOST–440181 (Izd. Standartov, Moscow, 1981), 179 pp.
9. L.T. Matveev, *Handbook on General Meteorology. Atmospheric Physics* (Gidrometeoizdat, Leningrad, 1984), 751 pp.

10. M.S. Belen'kii, G.O. Zadde, V.S. Komarov, et al., *Optical Atmospheric Model* (Tomsk Affiliate of the Siberian Branch of the Academy of Sciences of the USSR, Tomsk, 1987), 225 pp.
11. M.E. Gracheva and A.S. Gurvich, Izv. Akad. Nauk SSSR, Fiz. Atmos. Okeana **16**, 1107–1110 (1980).
12. A.A. Mitsel' and Yu.N. Ponomarev, *Optical Models of the Molecular Atmosphere* (Nauka, Novosibirsk, 1988), 127 pp.
13. V.E. Zuev and G.M. Krekov, *Optical Models of the Atmosphere* (Gidrometeoizdat, Leningrad, 1986), 256 pp.